Importance sampling and theory of nonequilibrium solvation dynamics in water

Cite as: J. Chem. Phys. **113**, 9759 (2000); https://doi.org/10.1063/1.1290136
Submitted: 05 May 2000 . Accepted: 10 July 2000 . Published Online: 16 November 2000

Phillip L. Geissler, and David Chandler

Importance sampling and theory of nonequilibrium solvation dynamics in water

Phillip L. Geissler and David Chandler[a)]
Department of Chemistry, University of California, Berkeley, California 94720

(Received 5 May 2000; accepted 10 July 2000)

We have devised a novel importance sampling method for nonequilibrium processes. Like transition path sampling, the method employs a Monte Carlo procedure to confine or bias the search through trajectory space. In this way, molecular dynamics trajectories consistent with the nonequilibrium dynamics of interest are generated efficiently. Using results of this sampling, we demonstrate that statistics of the energy gap between a solute's electronic states are Gaussian throughout the dynamics of nonequilibrium solvation in water. However, these statistics do change in time, reflecting linear response that is nonstationary. Discrepancies observed between the dynamics of nonequilibrium relaxation and of equilibrium fluctuations are thus explained. We analyze a simple Gaussian field theory that accounts for this nonstationary response. © *2000 American Institute of Physics.* [S0021-9606(00)52137-0]

I. INTRODUCTION

This article describes a method for carrying out importance sampling of nonequilibrium trajectories. It thus shows how biasing techniques commonly employed in the realm of equilibrium statistics, such as umbrella sampling, can be extended to the dynamical realm. The method we present may be applied to any nonequilibrium process for which a distribution of initial conditions is known. An important class of such processes is the relaxation following a sudden change in the Hamiltonian of a system that is initially at equilibrium.

In developing this sampling technique, we are motivated by an interest in the specific nonequilbrium phenomenon known as solvation dynamics,[1,2] and it is with this process that we illustrate our general approach. A solvation dynamics experiment measures the response of a polar solvent to an electronic transition of a solute. Because such transitions typically involve changes in the solute's charge distribution, surrounding solvent molecules are subject to large net forces and reorganize quickly. The dynamics of this response is monitored through a function

$$S(t) \equiv \frac{\overline{\Delta E}(t) - \overline{\Delta E}(\infty)}{\overline{\Delta E}(0) - \overline{\Delta E}(\infty)}. \tag{1}$$

Here, ΔE is the energy gap between ground and excited states, determined experimentally by fluorescence spectroscopy.[3,4] Overbars denote a nonequilibrium average, i.e., a Boltzmann-weighted sum over initial conditions with the solute in its ground state and with dynamics evolved in the excited state. $S(t)$ thus measures the normalized relaxation of the energy gap to its new equilibrium value, $\overline{\Delta E}(\infty)$.

Remarkably, it has been observed in molecular dynamics simulations that $S(t)$ is often nearly identical to an equilibrium time correlation function:[4,5]

$$C(t) \equiv \frac{\langle \delta\Delta E(t)\, \delta\Delta E(0)\rangle}{\langle (\delta\Delta E)^2\rangle}. \tag{2}$$

Here, angled brackets denote an equilibrium average with the solute in either its ground or excited electronic state. $\delta\Delta E$ is the fluctuation of the energy gap away from its average value at equilibrium, i.e., $\delta\Delta E \equiv \Delta E - \langle \Delta E\rangle$. The near equivalence of nonequilibrium relaxation dynamics and those of equilibrium fluctuations suggests that linear response is approximately valid for these solutions. Furthermore, the statistics of the energy gap at equilibrium, as determined by importance sampling in computer simulations, are remarkably Gaussian.[6] The corresponding harmonic free energy also suggests the validity of linear response. Until now, the statistics of the energy gap during nonequilibrium relaxation have not been determined by importance sampling. Consequently, these time-dependent distributions have been computed only for small fluctuations of the energy gap away from its mean.[7]

Although linear response appears to describe solvation dynamics for some systems, several workers have noted that $S(t)$ can differ significantly from $C(t)$ for others,[8–10] particularly those involving hydrogen-bonding solvents. A major conclusion of our work is that these differences are not necessarily due to a failure of linear response or of Gaussian statistics. Indeed, as we show explicitly for a model examined by Skaf and Ladanyi,[8] nonequilibrium relaxation is governed largely by Gaussian statistics, but these statistics are not stationary. To an excellent approximation, it is the deviation from stationarity that produces the differences between $S(t)$ and $C(t)$.

In determining the statistics of the energy gap during solvent response, we make use of an importance sampling in trajectory space. The method is analogous to transition path sampling of rare but important events, in that trajectories are harvested using a Monte Carlo procedure, as described in Sec. II. In this procedure, trajectories are displaced by chang-

a)Electronic mail: chandler@cchem.berkeley.edu

ing atomic momenta at a particular time and integrating equations of motion to obtain a different but similar path. Trial paths so obtained are accepted with a probability that reproduces a desired distribution of trajectories. This scheme thus allows a bias or constraint to be applied to the *sampling* of trajectories evolving in time with the system's natural, unbiased dynamics. Using such constraints, we compute the probability of observing energy gap values over a wide range during nonequilibrium relaxation.

The distributions of the energy gap we determine, also described in Sec. II, are remarkably Gaussian throughout the solvation dynamics. The principal conclusions we draw from this fact can be captured by a simple Gaussian field theory, as illustrated in Sec. III. In this theory, the solvent environment is represented as a coarse-grained dielectric material, except where hydrogen bonds are formed to a solute. In such regions, the polarization oscillates in a harmonic potential that simulates these strong interactions. Upon solute excitation, the boundaries of linearly responding solvent regions change, so that the normal modes of solvent response are nonstationary.

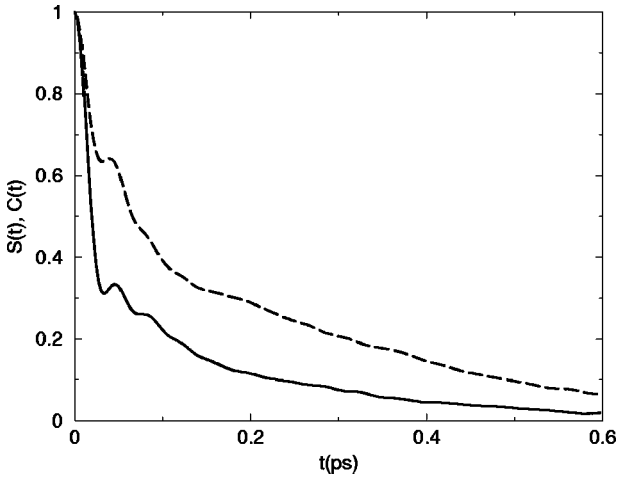

FIG. 1. Nonequilibrium response $S(t)$ (solid line) and equilibrium time correlation $C(t)$ (dashed line) as functions of time t for a dipolar solute in water. $S(t)$ was computed from 5000 nonequilibrium molecular dynamics trajectories. $C(t)$ was computed from a single, 1 ns trajectory at equilibrium.

II. NONEQUILIBRIUM MOLECULAR DYNAMICS

A. Sampling trajectories

The nonequilibrium average of the energy gap during relaxation to equilibrium may be computed using straightforward molecular dynamics. Long equilibrium trajectories with the solute in its ground electronic state are first used to generate initial configurations. For each configuration, the solute charge distribution is then switched instantaneously, and the energy gap is calculated as the solvent relaxes to equilibrium with the new electric field. Averaging over many of these trajectories yields $\overline{\Delta E}(t)$. Using this scheme, we have reproduced the results of Skaf and Ladanyi for a dipolar diatomic in liquid water whose ground and excited states are related by dipole inversion. The details of our simulations are nearly identical to those in Ref. 8 for a small solute (with opposite charges of $0.5e$ separated by ~ 3.1 Å) in TIP4P water. Both $S(t)$ and $C(t)$ are plotted in Fig. 1. Nonequilibrium relaxation indeed occurs much more quickly than is predicted by the dynamics of equilibrium fluctuations.

The above scheme of harvesting nonequilibrium trajectories does not allow efficient calculation of the distribution of energy gaps, $P[\Delta E(t)]$. In particular, only the most probable values of $\Delta E(t)$ are sampled frequently, while values lying in the wings of the distribution are rarely observed. In sampling the corresponding equilibrium distribution, $P[\Delta E(0)]$, this problem may be overcome by umbrella sampling. An artificial potential $\phi(\Delta E)$ is introduced, favoring improbable values of ΔE, so that the range of energy gaps is sampled with nearly even probability. Correcting for the bias imposed by $\phi(\Delta E)$ simply involves multiplication by a Boltzmann factor, $\exp[\beta(\phi(\Delta E))]$, where $\beta^{-1}=k_{\mathrm{B}}T$ is temperature multiplied by Boltzmann's constant. In practice, umbrella sampling is often accomplished by dividing the range of ΔE into overlapping windows. The distribution of ΔE is measured in each window, and the entire distribution is constructed by requiring that $P[\Delta E(0)]$ is continuous.

Such an umbrella potential does not, however, directly aid in the calculation of the nonequilibrium distribution. The artificial force that is introduced by $\phi(\Delta E)$ alters the dynamics of relaxation, and correcting for this effect is not straightforward. Rather than apply such a physical bias force to the system, we instead perform umbrella sampling in trajectory space in a manner analogous to the window sampling described above. The range of energy gaps at time t is divided into overlapping windows, defined by intervals $\Delta E^{(i)}_{\min} < \Delta E(t) < \Delta E^{(i)}_{\max}$. By computing $P[\Delta E(t)]$ in each window and requiring that the distribution is continuous at the window boundaries, we may efficiently sample a wide range of $\Delta E(t)$.

We harvest nonequilibrium trajectories in each window in a Monte Carlo fashion, as is done in transition path sampling of rare but important events.[11–13] Specifically, a trial trajectory is generated from an existing one and is accepted with a probability determined by the relative weight of the two trajectories. In detail, the weight of a trajectory in window i is

$$f^{(i)}(x_0) \propto e^{-\beta \mathcal{H}_{\mathrm{g}}(x_0)} h^{(i)}[\Delta E(t)] \tag{3}$$

$$\propto e^{-\beta \mathcal{H}_{\mathrm{e}}(x_0)} e^{\beta \Delta E(0)} h^{(i)}[\Delta E(t)]. \tag{4}$$

Here, $\mathcal{H}_{\mathrm{g}}(x_0)$ and $\mathcal{H}_e(x_0)$ are Hamiltonians with the solute in its ground and excited electronic states, respectively. $h^{(i)}[\Delta E(t)]$ is the characteristic function for window i:

$$h^{(i)}[\Delta E(t)] = \begin{cases} 1, & \text{if } \Delta E^{(i)}_{\min} < \Delta E(t) < \Delta E^{(i)}_{\max}, \\ 0, & \text{otherwise.} \end{cases} \tag{5}$$

In Eq. (4), x_t denotes the phase space point of the system at time t. Because the molecular dynamics we consider are Newtonian, the initial phase space point x_0 determines the state of the system at all later times. The trajectory weight $f^{(i)}$ is thus written as a function solely of x_0.

To sample trajectories consistent with the weight in Eq. (4), it is sufficient to satisfy the condition of detailed balance,

$$P_{\mathrm{gen}}(x_0^{\mathrm{o}}\to x_0^{\mathrm{n}})P_{\mathrm{acc}}(x_0^{\mathrm{o}}\to x_0^{\mathrm{n}})f^{(i)}(x_0^{\mathrm{o}}) = P_{\mathrm{gen}}(x_0^{\mathrm{n}}\to x_0^{\mathrm{o}})P_{\mathrm{acc}}(x_0^{\mathrm{n}}\to x_0^{\mathrm{o}})f^{(i)}(x_0^{\mathrm{n}}). \quad (6)$$

Here, $P_{\mathrm{gen}}(x_0^{\mathrm{o}}\to x_0^{\mathrm{n}})$ is the probability of generating a trial trajectory with initial conditions x_0^{n} from an old trajectory with initial conditions x_0^{o}. $P_{\mathrm{acc}}(x_0^{\mathrm{o}}\to x_0^{\mathrm{n}})$ is the probability that this new trajectory will be accepted. We use the Metropolis acceptance probability,

$$P_{\mathrm{acc}}(x_0^{\mathrm{o}}\to x_0^{\mathrm{n}}) = \min\left[1, \frac{f^{(i)}(x_0^{\mathrm{n}})}{f^{(i)}(x_0^{\mathrm{o}})}\frac{P_{\mathrm{gen}}(x_0^{\mathrm{n}}\to x_0^{\mathrm{o}})}{P_{\mathrm{gen}}(x_0^{\mathrm{o}}\to x_0^{\mathrm{n}})}\right], \quad (7)$$

which satisfies detailed balance by construction and does not require knowledge of the proportionality constant in Eq. (4).

In our Monte Carlo sampling, new trajectories are generated from old ones by an effective displacement in trajectory space, using shooting moves similar to those described in Ref. 14. A time step along the existing path is first chosen at random. The momentum of each atom is shifted at that time step by an amount $\delta\mathbf{p}_i$. Equations of motion are then integrated forwards and backwards in time, yielding a distinct trial path.

In the present work, the trajectories of interest are only tens of femtoseconds in duration. [The deviation of $S(t)$ from $C(t)$ is greatest at these times.] Consequently, large momentum displacements are necessary to generate trial trajectories that are not too similar to existing ones. If the $\delta\mathbf{p}_i$ are too small, sampling of statistically independent trajectories will occur slowly. However, if large $\delta\mathbf{p}_i$ are drawn from a symmetric distribution, high kinetic energies will often result. Trial paths will then be frequently rejected due to small values of $\exp[-\beta\mathcal{H}_e(x_0^{\mathrm{n}})]$. We avoid this sampling problem by effectively selecting the $\delta\mathbf{p}_i$ from an asymmetric distribution, as described in the Appendix. The corresponding path generation probabilities automatically reproduce a Boltzmann distribution of initial conditions:

$$\frac{P_{\mathrm{gen}}(x_0^{\mathrm{o}}\to x_0^{\mathrm{n}})}{P_{\mathrm{gen}}(x_0^{\mathrm{n}}\to x_0^{\mathrm{o}})} = \exp[-\beta[\mathcal{H}_{\mathrm{e}}(x_0^{\mathrm{n}}) - \mathcal{H}_{\mathrm{e}}(x_0^{\mathrm{o}})]]. \quad (8)$$

Trial paths must therefore be accepted according to

$$P_{\mathrm{acc}}(x_0^{\mathrm{o}}\to x_0^{\mathrm{n}}) = \min[1, e^{\beta[\Delta E^{\mathrm{n}}(0) - \Delta E^{\mathrm{o}}(0)]}h^{(i)}[\Delta E^{\mathrm{n}}(t)]. \quad (9)$$

Here, $\Delta E^{\mathrm{n}}(0)$ and $\Delta E^{\mathrm{o}}(0)$ denote the energy gaps at time zero for the new and old trajectories, respectively. We have assumed that $h^{(i)}[\Delta E^{\mathrm{o}}(t)]=1$, i.e., that the initial path lies within window i.

In practice, this sampling of nonequilibrium paths follows a simple algorithm. From an existing path, momenta are displaced at a randomly selected time, and a trial trajectory is obtained by integrating equations of motion. By Eq. (9), the trajectory is rejected if a random number between 0 and 1 is smaller than $e^{\beta[\Delta E^{\mathrm{n}}(0) - \Delta E^{\mathrm{o}}(0)]}$. Otherwise, it is accepted, *provided* $\Delta E(t)$ lies within the interval defined by the current window. This final condition makes our sampling efficient. It allows us to control the range of $\Delta E(t)$ sampled, while maintaining the appropriate distribution of initial conditions.

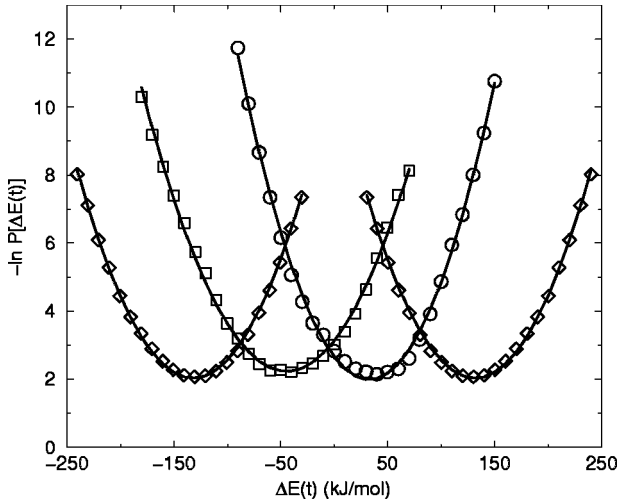

FIG. 2. Natural logarithm of the energy gap distribution $P[\Delta E(t)]$ at four times during nonequilibrium relaxation following the solute's dipolar transition. The rightmost curve (diamonds) corresponds to $t=0$, i.e., the initial equilibrium distribution. The leftmost curve (also diamonds) corresponds to $t=\infty$, and is by symmetry a reflection of the $t=0$ result about the vertical axis. These two results were computed from long equilibrium trajectories. The middle two curves correspond to intermediate times $t_1=15$ fs (circles) and $t_2=30$ fs (squares). These nonequilibrium results were obtained using the importance sampling described in Sec. II. Best-fit parabolas (solid lines) are plotted for each curve. Symbols are approximately the size of average statistical uncertainties estimated through block averages.

In principle, this efficient sampling can be applied to any nonequilibrium process when the appropriate distribution of initial conditions is known.

B. Nonequilibrium statistics of the energy gap

Using this importance sampling, we have computed the distribution of energy gaps at two times during the nonequilibrium relaxation. In both cases, we harvested about 10^5 trajectories in each window. (The width of a window is about 30 kJ/mol.) In Fig. 2, we have plotted $\rho(t) = -\ln(P[\Delta E(t)])$, an effective free energy in units of $k_{\mathrm{B}}T$, for times $t_1=15$ fs and $t_2=30$ fs. Equilibrium free energies for the two solute states, corresponding to $\rho(0)$ and $\rho(\infty)$, are plotted alongside for comparison. At both t_1 and t_2, $\rho(t)$ is statistically indistinguishable from a best-fit parabola (also plotted in Fig. 2) over the entire range considered. The statistics of the energy gap are thus Gaussian to a remarkable extent, even for fluctuations 5000 times less probable than the average value. Nonlinearities, which would result in anharmonicity of $\rho(t)$, are not apparent in our results.

While the nonequilibrium distributions we have computed are remarkably Gaussian, their variances differ from those of the equilibrium distributions. Specifically, the root mean square fluctuation of $\Delta E(t)$ away from its mean, $\overline{\Delta E}(t)$, is 28 kJ/mol at time t_1 and 33 kJ/mol at t_2. At equilibrium, $\langle\delta(\Delta E)^2\rangle^{1/2}$ is 31 kJ/mol. These variances, or equivalently the curvature of $\rho(t)$, reflect the susceptibility of the system to an applied field. Their time dependence therefore indicates that the Green's function $G(t;t')$, which describes the response of the system at time t to a perturbation at time t', does not depend simply on the difference t

$-t'$. This nonstationary property reflects normal modes that change in time.

The normal modes of aqueous response to an applied electric field may be pictured most simply as those of a dielectric medium. This approximation has been successful in a broad range of applications, including Marcus's theory of electron transfer[15] and in several theories of solvation dynamics.[16,17] Dielectric response is very sensitive, however, to boundary conditions. Indeed, the presence of a solute can significantly alter the normal modes of a dielectric by expelling the solvent from a region of space.[18] Consequently, a perturbation that changes the boundary conditions of a dielectric in time will give rise to a nonstationary response. An example of such a perturbation is a change in the solvent-excluding volume of a solute.

In the solute transition considered by Skaf and Ladanyi, the effective size and shape of the solute do not change. The equilibrium density of oxygen atoms surrounding the dipolar solute indicates that water molecules are distributed nearly equivalently about the two atoms comprising the solute. The density of hydrogen atoms, on the other hand, shows a sharp discrepancy in solvation of the two solute atoms. As Skaf and Ladanyi observed, water molecules form strong hydrogen bonds to the negatively charged atom that are broken only rarely, resulting in close hydrogen–negative-atom contacts (~ 2 Å). These close contacts are of course not present around the positively charged atom. Because the water molecules engaging in these hydrogen bonds are tightly bound, their response to an electric field is expected to differ from that of bulk water. When the dipole is inverted, the location of this hydrogen bonding region changes suddenly, changing also the boundary of the solvent region that behaves as a dielectric. This change of boundary conditions can account for the nonstationary nature of solvent response we have computed, a possibility we examine in the next section.

III. GAUSSIAN FIELD THEORY

The Gaussian statistics of the energy gap described in Sec. II suggest that the nonequilibrium response $S(t)$ may be understood by applying linear response theory appropriately. We consider here a harmonic model of solvent dynamics, with normal modes that change upon solute excitation. Specifically, we imagine that when the solute exerts a weak electric field, the solvent may be represented as a dielectric, i.e., as a coarse-grained polarizable medium expelled from the solute. However, when the solute exerts a strong electric field, the solvent must be partitioned into an inner shell region (''IS''), in which strong hydrogen bonds to the solute are formed, and an external dielectric region (''out''). Using this model, we analyze an experiment similar to that considered by Skaf and Ladanyi. (See Fig. 3.) For times $t<0$, the solute exerts no electric field. At time $t=0$, a collection of n solute dipoles μ_i is turned on, generating a nonequilibrium response.

The dynamics of solvent relaxation in our model are determined by the Hamiltonian

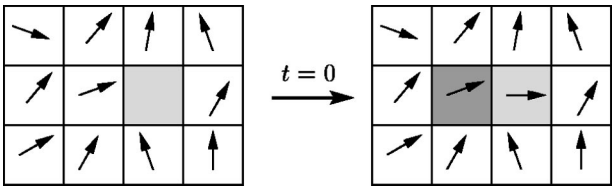

FIG. 3. Example geometry for the model analyzed in Sec. III. The lightly shaded lattice cell represents the solute. The inner shell region, adjacent to the solute, is more darkly shaded. A few lattice cells belonging to the dielectric are shown unshaded. Arrows depict coarse-grained dipole density. For times $t<0$, the solute exerts no electric field and no inner shell exists. At $t=0$, a solute dipole is created, and an adjacent cell becomes the inner shell.

$$\mathcal{H}=\mathcal{H}_0(\{\mathbf{m}_\mathbf{r}\}_{\mathrm{IS}})-\sum_{i=1}^{n}\mu_i\cdot\mathbf{F}_{\mathbf{r}_i}-\sum_{\mathbf{r}\in\mathrm{IS}}\mathbf{m}_\mathbf{r}\cdot\mathbf{F}_\mathbf{r}+\mathcal{H}_{\mathrm{D}}(\{\mathbf{m}_\mathbf{r}\}_{\mathrm{out}}),\ t>0, \tag{10}$$

where

$$\mathcal{H}_0=\frac{M}{2}\sum_{\mathbf{r}\in\mathrm{IS}}\left[|\dot{\mathbf{m}}_\mathbf{r}|^2+\omega^2|\mathbf{m}_\mathbf{r}-\mathbf{m}_\mathbf{r}^{(0)}|^2\right]+\frac{1}{2}\sum_{\mathbf{r}\in\mathrm{IS}}\sum_{\mathbf{r}'(\neq\mathbf{r})\in\mathrm{IS}}\mathbf{m}_\mathbf{r}\cdot\nabla\nabla'\frac{1}{|\mathbf{r}-\mathbf{r}'|}\cdot\mathbf{m}_{\mathbf{r}'}+\sum_{i=1}^{n}\sum_{\mathbf{r}\in\mathrm{IS}}\mu_i\cdot\nabla_i\nabla'\frac{1}{|\mathbf{r}_i-\mathbf{r}'|}\cdot\mathbf{m}_\mathbf{r}, \tag{11}$$

and

$$\mathbf{F}_\mathbf{r}=-\sum_{\mathbf{r}'\ \mathrm{out}}\nabla\nabla'\frac{1}{|\mathbf{r}-\mathbf{r}'|}\cdot\mathbf{m}_{\mathbf{r}'}. \tag{12}$$

Here, $\mathbf{m}_\mathbf{r}$ denotes the solvent dipole density at lattice position $\mathbf{r}$, which takes on discrete lattice values. In the inner shell region, the $\mathbf{m}_\mathbf{r}$ are harmonic oscillators with potential energy $\frac{1}{2}M\omega^2|\mathbf{m}_\mathbf{r}-\mathbf{m}_\mathbf{r}^{(0)}|^2$, mimicking the effects of strong hydrogen bonds. Here, M is an effective mass for the oscillators, ω is their frequency, and $\mathbf{m}_\mathbf{r}^{(0)}$ is their average value in the absence of other interactions. $\mathcal{H}_{\mathrm{D}}(\{\mathbf{m}_\mathbf{r}\})$ is the Hamiltonian for a coarse-grained homogeneous dielectric, expelled from the solute and from the inner shell. The solute, inner shell, and dielectric are coupled through dipole–dipole interactions. For lattice cell separation vectors $\mathbf{r}\neq\mathbf{r}'$, the dipole interaction tensor has the usual form:

$$\nabla\nabla'\frac{1}{|\mathbf{r}-\mathbf{r}'|}=\frac{\mathbf{I}}{|\mathbf{r}-\mathbf{r}'|^3}-3\frac{(\mathbf{r}-\mathbf{r}')(\mathbf{r}-\mathbf{r}')}{|\mathbf{r}-\mathbf{r}'|^5},\ \mathbf{r}\neq\mathbf{r}'. \tag{13}$$

Because dipole density is coarse-grained in our model, the interactions described by Eq. (13) are only approximately correct. In the manipulations that follow, we take the singularity at $\mathbf{r}=\mathbf{r}'$ to be coarse grained over a single lattice cell:

$$\nabla\nabla'\frac{1}{|\mathbf{r}-\mathbf{r}'|}=\frac{4\pi\rho}{3}\mathbf{I},\ \mathbf{r}=\mathbf{r}'. \tag{14}$$

We solve for the dynamics of relaxation by first integrating out the dielectric. The time dependence of the resulting force $\mathbf{F}_\mathbf{r}$ on the remaining degrees of freedom is determined by linear response.[19] In detail,

$$\mathbf{F}_{\mathbf{r}}(t)=\mathbf{F}_{\mathbf{r}}^{(\mathrm{D})}(t)+\int_0^t dt'\left[\sum_{i=1}^{n}\mathbf{X}^{(\mathrm{D})}(\mathbf{r},\mathbf{r}_i;t-t')\cdot\mu_i+\sum_{\mathbf{r}'\in\mathrm{IS}}\mathbf{X}^{(\mathrm{D})}(\mathbf{r},\mathbf{r}';t-t')\cdot\mathbf{m}_{\mathbf{r}'}(t')\right]. \tag{15}$$

The superscript (D) in Eq. (15) denotes time evolution according to $\mathcal{H}_{\mathrm{D}}(\{\mathbf{m}_{\mathbf{r}}\}_{\mathrm{out}})$ alone. In particular,

$$\mathbf{X}^{(\mathrm{D})}(\mathbf{r},\mathbf{r}';t-t')=\sum_{\mathbf{r}'',\mathbf{r}'''\mathrm{out}}\nabla\nabla''\frac{1}{|\mathbf{r}-\mathbf{r}''|}\cdot\chi^{(\mathrm{m})}(\mathbf{r},\mathbf{r}';t-t')\cdot\nabla'''\nabla'\frac{1}{|\mathbf{r}'''-\mathbf{r}'|}, \tag{16}$$

where

$$\chi^{(\mathrm{m})}(\mathbf{r},\mathbf{r}';t-t')=-\beta\frac{d}{d(t-t')}\langle\mathbf{m}_{\mathbf{r}}(t)\mathbf{m}_{\mathbf{r}'}(t')\rangle_{\mathrm{D}} \tag{17}$$

is the dielectric susceptibility. Exclusion from the solute and inner shell region (collectively, the ''in'' region) modifies this susceptibility from that of a uniform dielectric. In this case, modification is given by Chandler's formula[18,20]

$$\tilde{\chi}^{(\mathrm{m})}(\mathbf{r},\mathbf{r}';s)=\chi(\mathbf{r}-\mathbf{r}';s)-\sum_{\mathbf{r}'',\mathbf{r}'''\mathrm{in}}\tilde{\chi}(\mathbf{r}-\mathbf{r}'';s)\cdot\tilde{\chi}_{\mathrm{in}}^{-1}(\mathbf{r}'',\mathbf{r}''';s)\cdot\tilde{\chi}(\mathbf{r}'''-\mathbf{r}';s), \tag{18}$$

where

$$\tilde{\chi}(\mathbf{r}-\mathbf{r}';s)=\frac{\epsilon-1}{4\pi\rho}\left[\delta_{\mathbf{r},\mathbf{r}'}\mathbf{I}-\frac{\epsilon-1}{4\pi\rho\epsilon}\nabla\nabla'\frac{1}{|\mathbf{r}-\mathbf{r}'|}\right]. \tag{19}$$

Here, $\tilde{f}(s)$ denotes the Laplace transform of $f(t)$:

$$\tilde{f}(s)=\int_0^\infty dt\, e^{-st}f(t). \tag{20}$$

The susceptibility in Eq. (19) has been shown to reproduce the phenomenology of a dielectric continuum with dispersion $\epsilon(s)$ and dipole density ρ.[19] In Eq. (18), $\tilde{\chi}_{\mathrm{in}}^{-1}$ is the inverse of the uniform susceptibility over the ''in'' region. Substituting Eqs. (18) and (19) into the Laplace transform of Eq. (16) and simplifying, we obtain

$$\tilde{\mathbf{X}}^{(\mathrm{D})}(\mathbf{r},\mathbf{r}';s)=\frac{4\pi\rho}{\epsilon-1}\delta_{\mathbf{r},\mathbf{r}'}\mathbf{I}+\nabla\nabla'\frac{1}{|\mathbf{r}-\mathbf{r}'|}-\tilde{\chi}_{\mathrm{in}}^{-1}(\mathbf{r},\mathbf{r}';s). \tag{21}$$

In arriving at Eq. (21), we have repeatedly used the identities

$$\sum_{\mathbf{r}''}\nabla\frac{1}{|\mathbf{r}-\mathbf{r}''|}\cdot\tilde{\chi}(\mathbf{r}'',\mathbf{r}';s)=\frac{\epsilon-1}{4\pi\rho\epsilon}\nabla\frac{1}{|\mathbf{r}-\mathbf{r}'|} \tag{22}$$

and

$$\sum_{\mathbf{r}''\mathrm{in}}\nabla\nabla''\frac{1}{|\mathbf{r}-\mathbf{r}''|}\cdot\tilde{\chi}_{\mathrm{in}}^{-1}(\mathbf{r}'',\mathbf{r}';s)=\frac{4\pi\rho\epsilon}{\epsilon-1}\tilde{\chi}_{\mathrm{in}}^{-1}(\mathbf{r},\mathbf{r}';s)-\left(\frac{4\pi\rho}{\epsilon-1}\right)^2\epsilon\delta_{\mathbf{r},\mathbf{r}'}\mathbf{I}. \tag{23}$$

The first identity may be proven using spatial Fourier transforms. The second follows from the definition of $\tilde{\chi}_{\mathrm{in}}^{-1}$. Equations (15) and (21) determine, in a computationally manageable form, the influence of dielectric response on the solute and inner shell dipoles.

With the dynamics of the dielectric determined implicitly through Eq. (15), closed equations of motion for the inner shell dipoles may be written:

$$M\ddot{\mathbf{m}}_{\mathbf{r}}(t)=-\frac{\partial\mathcal{H}_0}{\partial\mathbf{m}_{\mathbf{r}}}+\mathbf{F}_{\mathbf{r}}(t). \tag{24}$$

Substituting $\mathcal{H}_0$ from Eq. (11), taking Laplace transforms, and averaging over initial conditions yields

$$M(s^2+\omega^2)\overline{\tilde{\mathbf{m}}_{\mathbf{r}}(s)}=\frac{M\omega^2}{s}\mathbf{m}_{\mathbf{r}}^{(0)}+\sum_{\mathbf{r}'\in\mathrm{IS}}\left[(\delta_{\mathbf{r},\mathbf{r}'}-1)\nabla\nabla'\frac{1}{|\mathbf{r}-\mathbf{r}'|}+\tilde{\mathbf{X}}^{(\mathrm{D})}(\mathbf{r},\mathbf{r}';s)\right]\cdot\overline{\tilde{\mathbf{m}}_{\mathbf{r}'}(s)}+\sum_{i=1}^{n}\left[-\nabla\nabla_i\frac{1}{|\mathbf{r}-\mathbf{r}_i|}+\tilde{\mathbf{X}}^{(\mathrm{D})}(\mathbf{r},\mathbf{r}_i;s)\right]\cdot\frac{1}{s}\mu_i. \tag{25}$$

Equation (25) determines a set of coupled linear equations for the dynamics of the inner shell dipoles $\overline{\tilde{\mathbf{m}}_{\mathbf{r}}(s)}$ that may be solved by matrix inversion. Having thus evaluated the solvent dynamics, we may compute the average energy gap according to

$$\overline{\widetilde{\Delta E}(s)}=\sum_{i=1}^{n}\mu_i\cdot\left[\sum_{\mathbf{r}\in\mathrm{IS}}\nabla_i\nabla\frac{1}{|\mathbf{r}_i-\mathbf{r}|}\cdot\overline{\tilde{\mathbf{m}}_{\mathbf{r}}(s)}-\overline{\tilde{\mathbf{F}}_{\mathbf{r}_i}(s)}\right]. \tag{26}$$

Using Eq. (26), we have calculated $S(t)$ for the simple solute and inner shell geometry depicted in Fig. 3. The solute occupies a single lattice cell and, for $t>0$, possesses a dipole $\mu=\mu_0\hat{a}$ parallel to the lattice vector $\hat{a}$. When this dipole is created at time $t=0$, the solvent dipole nearest to the negative end of the solute becomes the inner shell, with $\mathbf{m}^{(0)}=(2\mathrm{D})\hat{a}$, $\omega=1.3\times10^{14}\,\mathrm{s}^{-1}$ (corresponding to a librational frequency in water), and a mass M consistent with the rotational inertia of a water molecule. We used a lattice spacing of 5 Å and dielectric data for water determined by Neumann from molecular dynamics.[21] Laplace transforms in Eq. (26) were inverted numerically, using the algorithm of Stehfest.[22] $S(t)$ so obtained is plotted in Fig. 4, as is $C(t)$ for fluctuations in the ground state. $C(t)$ was computed for dipole solvation energy fluctuations with the initial geometry in Fig. 3. (This calculation is described in Ref. 18.) The qualitative features of these functions, as predicted by our model, are similar to those obtained from molecular dynamics. In particular, $S(t)$ decays much more quickly than $C(t)$ during the first 50 fs. Thereafter, $S(t)$ and $C(t)$ decay with roughly the same time constant, reflecting slower modes of dielectric relaxation that are not strongly affected by the changing boundary conditions.

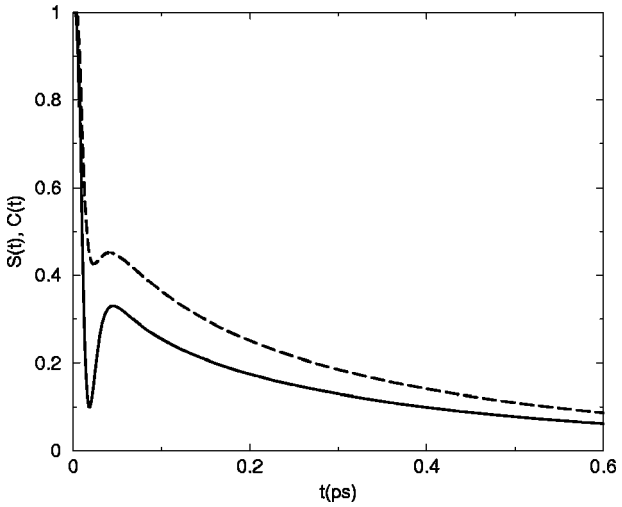

FIG. 4. $S(t)$ (solid line) and $C(t)$ (dashed line) determined by our Gaussian field theory, as functions of time t following the solute transition depicted in Fig. 3. $S(t)$ was computed from Eqs. (1) and (26). $C(t)$ was computed using Eq. 5.7 of Ref. 19.

IV. CONCLUSIONS

We have shown that an example of apparently nonlinear response can be understood in terms of linear response theory, if correctly applied. For a dipolar transition in a small solute in water, the distribution of energy gaps is Gaussian during nonequilibrium relaxation, even for large fluctuations away from the mean. We have demonstrated this fact using a novel importance sampling of nonequilibrium dynamics. The time-dependent variance of energy gaps evidently reflects the cleavage and formation of hydrogen bonds to the solute. The principal effect of this rearrangement is to modify the boundaries of solvent regions that are inherently linearly responding. Because normal modes change as a result, the expectation that $S(t)=C(t)$ is no longer correct, even though the system does respond linearly. We have shown that a simple, harmonic model can in fact reproduce the qualitative features of both equilibrium fluctuations and nonequilibrium relaxation.

Note added in proof. Because dynamics are linear in our Gaussian field theory, the corresponding nonequilibrium distribution of energy gaps is completely characterized by its mean [Eq. (26)] and variance. We have determined this variance for the geometry shown in Fig. 3 using techniques similar to those employed above. During the relaxation induced by the solute's electric field and changing boundary conditions, $[\overline{(\delta\Delta E)^2}(t)]^{1/2}$ for the simple model changes by more than 100% of its initial value.[23] By contrast, the variance determined from our molecular dynamics simulations changes by only 10% over this period. (See Fig. 2.) Our simple model thus exaggerates the nonstationary character of the solvation dynamics. The variance of energy gap fluctuations is not, however, truly a force constant for energy gap dynamics, and does not directly determine $S(t)$. Rather, these dynamics are governed by a complicated collection of interactions: couplings among dipole densities in our Gaussian field theory, and long-ranged interatomic forces in our molecular dynamics simulations. We therefore expect that a more detailed Gaussian theory can account for the apparently nonlinear response without a large change in the variance of energy gap fluctuations.

ACKNOWLEDGMENTS

We benefitted from guidance and suggestions from Xueyu Song in the early stages of this work. P.L.G. was a National Science Foundation Predoctoral Fellow. This research has been supported by the Office of Basic Energy Sciences, Chemical Sciences Division of the U. S. Department of Energy in its early stages with Grant No. DE-FG03-87ER13793 and in the later stages with Grant No. DE-FG03-99ER14987.

APPENDIX

In order to make large changes in momenta without correspondingly large changes in kinetic energy, we generate path displacements in a two-step process. First, a random displacement $\delta\mathbf{w}_i$ is added to the old mass-weighted momenta $\mathbf{w}_i^{\mathrm{o}}(t)$ of each atom i at time t, where

$$\mathbf{w}_i=\mathbf{p}_i/\sqrt{m_i}. \tag{A1}$$

The $\delta\mathbf{w}_i$ are chosen such that the total kinetic energy,

$$K^{\mathrm{o}}=\frac{1}{2}\sum_i |\mathbf{w}_i|^2, \tag{A2}$$

is unchanged, and the constraints of vanishing total linear momentum and rigid intramolecular bonds are maintained. (An algorithm for generating such a displacement is described in the Appendix of Ref. 14.) Second, a new kinetic energy is selected using a Monte Carlo procedure. A change in kinetic energy, δK, is chosen at random from a Gaussian distribution. The trial value $K^{\mathrm{t}}=K^{\mathrm{o}}+\delta K$ is accepted with probability

$$p_{\mathrm{acc}}=\min[1,P(K^{\mathrm{t}})/P(K^{\mathrm{o}})], \tag{A3}$$

where

$$P(K)\propto e^{-\beta K}K^{(n_f/2)-1} \tag{A4}$$

is the kinetic energy equilibrium distribution for a system with n_f degrees of freedom in contact with a heat bath at inverse temperature β. The mass-weighted momenta are then scaled to give the resulting kinetic energy K^{n}:

$$\mathbf{w}_i^{\mathrm{n}}=\left(\frac{K^{\mathrm{n}}}{K^{\mathrm{o}}}\right)^{1/2}(\mathbf{w}_i^{\mathrm{o}}+\delta\mathbf{w}). \tag{A5}$$

The result of this process is that a new path is generated from an old one with relative probability

$$\frac{P_{\mathrm{gen}}(x_0^{\mathrm{o}}\to x_0^{\mathrm{n}})}{P_{\mathrm{gen}}(x_0^{\mathrm{n}}\to x_0^{\mathrm{o}})}=\exp[-\beta(K^{\mathrm{n}}(t)-K^{\mathrm{o}}(t))], \tag{A6}$$

and with arbitrarily large displacements $\delta\mathbf{w}_i$. Because the potential energy is unchanged at time t, and because Newton's equations of motion conserve total energy, Eq. (A6) is equivalent to Eq. (8) in the text.

[1] B. Bagchi, D. W. Oxtoby, and G. R. Fleming, Chem. Phys. **86**, 257 (1984).
[2] E. W. Castner and M. Maroncelli, J. Mol. Liq. **77**, 1 (1998).
[3] M. Maroncelli, J. MacInnis, and G. R. Fleming, Science **243**, 1674 (1989).
[4] R. Jimenez, G. R. Fleming, P. V. Kumar, and M. Maroncelli, Nature (London) **369**, 471 (1994).
[5] J. S. Bader and D. Chandler, Chem. Phys. Lett. **157**, 501 (1989).
[6] R. A. Kuharski, J. S. Bader, D. Chandler, M. Sprik, M. L. Klein, and R. W. Impey, J. Chem. Phys. **89**, 3248 (1988).
[7] E. A. Carter and J. T. Hynes, J. Chem. Phys. **94**, 5961 (1991).
[8] M. S. Skaf and B. M. Ladanyi, J. Phys. Chem. **100**, 18258 (1996).
[9] T. Fonseca and B. M. Ladanyi, J. Mol. Liq. **60**, 1 (1994).
[10] M. Maroncelli and G. R. Fleming, J. Chem. Phys. **89**, 5044 (1988).
[11] C. Dellago, P. G. Bolhuis, F. S. Csajka, and D. Chandler, J. Chem. Phys. **108**, 1964 (1998).
[12] C. Dellago, P. G. Bolhuis, and D. Chandler, J. Chem. Phys. **108**, 9236 (1998).
[13] P. G. Bolhuis, C. Dellago, and D. Chandler, Faraday Discuss. **110**, 421 (1998).
[14] P. L. Geissler, C. Dellago, and D. Chandler, Phys. Chem. Chem. Phys. **1**, 1317 (1999).
[15] R. A. Marcus, J. Chem. Phys. **24**, 966 (1956).
[16] G. van der Zwan and J. T. Hynes, J. Phys. Chem. **89**, 4181 (1985).
[17] X. Song and D. Chandler, J. Chem. Phys. **108**, 2594 (1998).
[18] X. Song, D. Chandler, and R. A. Marcus, J. Phys. Chem. **100**, 11954 (1996).
[19] For example, D. Chandler, *Introduction to Modern Statistical Mechanics* (Oxford University Press, New York, 1987), Sec. 8.8.
[20] D. Chandler, Phys. Rev. E **48**, 2898 (1993); Y. Georgievskii, C.-P. Hsu, and R. A. Marcus, J. Chem. Phys. **110**, 5307 (1999).
[21] M. Neumann, J. Chem. Phys. **85**, 1567 (1986).
[22] H. Stehfest, Commun. ACM **13**, 47 (1970).
[23] P. L. Geissler, Ph.D. thesis, University of California, Berkeley.